

Electronic supplementary information:
Identifying key environmental objectives
for integrated process and fuel design

*Simon Voelker^a, Philipp Ackermann^b, Marcel Granderath^a, Clemens Kortmann^b, Joern Viell^b,
Alexander Mitsos^{c,b,d}, Niklas von der Assen^{c,a,*}*

^a Institute of Technical Thermodynamics, RWTH Aachen University, Aachen 52062, Germany

^b Process Systems Engineering, RWTH Aachen University, Aachen 52074, Germany

^c JARA-ENERGY, 52056 Aachen, GERMANY

^d Energy Systems Engineering (IEK-10), Forschungszentrum Jülich, Jülich 52425, Germany

* Corresponding author: niklas.vonderassen@itt.rwth-aachen.de

Table of contents

Note S1	Overview on recent applications of objective reduction methods.....	2
Note S2	Model description of integrated process and fuel design	3
Note S3	Exemplary minimization problem of objective reduction	6
Note S4	Comparison with previous fuel design studies	7
Note S5	Life cycle assessment: inventory data	8
Note S6	Influence of the number of Pareto points used as input for objective reduction.....	9
Note S7	Correlation matrices	10
Note S8	Optimal process and fuel designs for the reduced objective subset.....	11
Note S9	Contribution analysis	12
Note S10	Composition of Pareto-optimal bio-hybrid fuels	29
	Supplementary references.....	30

Note S1 Overview on recent applications of objective reduction methods

In Table S1, we give an overview on recent applications of objective reduction methods on environmental objectives. Approximately 70% of the case studies use the dominance-based objective reduction method by Guillén-Gosálbez et al.¹ that is based on the work of Brockhoff and Zitzler.² Correlation-based principal component analysis (PCA) is used by 33%, whereas 6% rely on other methods for objective reduction.

Table S1: Recent studies that applied objective reduction methods on environmental objectives. PCA: principal component analysis. Related to the Introduction.

Author	Year	Objective reduction method			Application
		Dominance	PCA	Other	
Qin et al. ³	2020		X		Energy systems
Chu et al. ⁴	2018		X		Tidal flat reclamation
Pérez-Gallardo et al. ⁵	2018		X		Photovoltaic grid-connected systems
Vázquez et al. ⁶	2018	X	X		Chemical supply chains
Vázquez et al. ⁶	2018	X	X		Construction of a building
Vázquez et al. ⁷	2018	X	X		Safety of a distillation train
Vázquez et al. ⁸	2018	X			Chemical supply chains
Vázquez et al. ⁸	2018	X			Construction of a building
Hennen et al. ⁹	2017	X			Energy system
Wheeler et al. ¹⁰	2017			X	Bioethanol supply chains
Carreras et al. ¹¹	2016	X			Construction of a building
Copado-Méndez et al. ¹²	2016	X			Bioethanol supply chains
Copado-Méndez et al. ¹²	2016	X			Hydrogen supply chains
Steinmann et al. ¹³	2016		X		Product life cycles
Kostin et al. ¹⁴	2015	X			Bioethanol supply chains
Kostin et al. ¹⁴	2015	X			Hydrogen supply chains
Postels et al. ¹⁵	2015	X			Energy system
Copado-Méndez et al. ¹⁶	2014	X			Hydrogen supply chains
Copado-Méndez et al. ¹⁶	2014	X			Metabolic networks
Čuček et al. ¹⁷	2014			X	Biomass and bioenergy supply chains
Vaskan et al. ¹⁸	2014	X			Utility plants
Antipova et al. ¹⁹	2013	X			Reverse osmosis desalination plant
Oliva et al. ²⁰	2013	X			Chemical supply chains
Oliva et al. ²⁰	2013	X			Bioethanol supply chains
Oliva et al. ²⁰	2013	X			Hydrogen supply chains
Brunet et al. ²¹	2012		X		L-lysine production
Kostin et al. ²²	2012	X			Bioethanol supply chains
Pozo et al. ²³	2012		X		Chemical supply chains
Sabio et al. ²⁴	2012		X		Hydrogen supply chains
Vaskan et al. ²⁵	2012	X			Heat exchanger
Guillén-Gosálbez et al. ¹	2011	X			Heat exchanger
Guillén-Gosálbez et al. ¹	2011	X			Chemical supply chains
Gutiérrez et al. ²⁶	2010		X		Domestic appliances

Note S2 Model description of integrated process and fuel design

Here, we briefly summarize the environmental and economical objective functions of König et al.^{27,28} In contrast to König et al., we write the environmental objective in a generalized form for an environmental impact (EI) instead of specifically for global warming impact. In Table S2, we list the 47 fuel species considered in this study.

The m th environmental impact per functional unit EI_m is calculated by dividing the total environmental impact $EI_{total,m}$ by a fixed annual fuel production of $\alpha = 2.77 \cdot 10^{12} \frac{\text{kJ}}{\text{a}}$. This annual fuel production relates to the energy content of 100,000 tons of ethanol per year, in line with previous studies.^{27–29}

$$EI_m = \frac{EI_{total,m}}{\alpha} \quad (S1)$$

The total environmental impact $EI_{total,m}$ comprises the impacts due to the supply of utilities $EI_{util,m}$ and feedstocks $EI_{feedstock,m}$:

$$EI_{total,m} = EI_{util,m} + EI_{feedstock,m} \quad (S2)$$

Environmental impacts due to utility supply $EI_{util,m}$ are calculated by multiplying the energy demands of reactions $E_{\text{reac},i}$ and separation sequences $E_{\text{sep},i}$ with the specific environmental impact factor $ei_{i,m}$ of the i th utility. Considered utilities are electricity, process heat, cooling, and refrigeration.

$$EI_{util,m} = \sum_{i \in N_{\text{utils}}} (E_{\text{reac},i} + E_{\text{sep},i}) \cdot ei_{i,m} \quad (S3)$$

Environmental impacts induced by feedstock supply $EI_{feedstock,m}$ are calculated as the product of the feedstock fluxes f_j , their molar masses M_j , and the specific environmental impact factor $ei_{j,m}$ of the j th feedstock. As feedstocks, we consider biomass, carbon dioxide, and hydrogen but also solvents (see Table S4).

$$EI_{feedstock,m} = \sum_{j \in N_{\text{feedstock}}} f_j M_j ei_{j,m} \quad (S4)$$

As economical objective, the production cost per functional unit C is evaluated by dividing the total annualized production cost C_{total} by the fixed annual fuel production α :

$$C = \frac{C_{\text{total}}}{\alpha} \quad (S5)$$

The total annualized production cost C_{total} is determined by summing up the annualized costs due to investments C_{invest} , utilities C_{util} , feedstocks $C_{\text{feedstock}}$, and wastes C_{waste} :

$$C_{\text{total}} = C_{\text{invest}} + C_{\text{util}} + C_{\text{feedstock}} + C_{\text{waste}} \quad (S6)$$

Annualized investment costs C_{invest} are calculated from the investment costs IC , the interest rate ir , and the project lifetime a :

$$C_{\text{invest}} = \frac{ir}{1 - (1 + ir)^{-a}} \cdot IC \quad (S7)$$

The investment costs IC are derived from the amount of transferred energy in reactions $E_{\text{reac,transfer},i}$ and separation sequences $E_{\text{sep,transfer},i}$ as well as the chemical engineering plant cost index (CEPCI) of the years 1993 and 2016, according to an empirical investment cost correlation.

$$IC = \frac{\text{CEPCI}_{2016}}{\text{CEPCI}_{1993}} \cdot 2.9 \cdot (E_{\text{transfer duty}})^{0.55} \quad (S8)$$

$$E_{\text{transfer duty}} = \sum_i (E_{\text{reac,transfer},i} + E_{\text{sep,transfer},i}) \quad (\text{S9})$$

Utility costs C_{util} are determined by multiplying the energy demands of reactions $E_{\text{reac},i}$ and separation sequences $E_{\text{sep},i}$ with the specific utility price parameter P_i :

$$C_{\text{util}} = \sum_{i \in N_{\text{utils}}} (E_{\text{reac},i} + E_{\text{sep},i}) \cdot P_i \quad (\text{S10})$$

Feedstock costs $C_{\text{feedstock}}$ are the product of the feedstock fluxes f_j , their molar masses M_j , and the specific feedstock price parameter P_j :

$$C_{\text{feedstock}} = \sum_{j \in N_{\text{feedstock}}} f_j M_j P_j \quad (\text{S11})$$

Waste costs C_{waste} are estimated by multiplying the fluxes of wastes w_k and byproducts b_k with their molar masses M_k and a generic waste price P_{waste} for liquid and solid wastes:

$$C_{\text{waste}} = \sum_{k \in N_{\text{waste}}} (w_k + b_k) M_k P_{\text{waste}} \quad (\text{S12})$$

Table S2: Fuel species considered in this study, adapted from König et al.²⁹

Fuel species	Fuel species (continued)
<i>alcohols</i>	<i>esters</i>
methanol	methyl acetate
ethanol	ethyl acetate
2-propanol	propyl acetate
1-butanol	isopropyl acetate
iso-butanol	butyl acetate
2-butanol	isobutyl acetate
3-butanol	ethyl propionate
n-pentanol	methyl butyrate
iso-pentanol	ethyl butyrate
2-pentanol	methyl isobutyrate
cyclopentanol	ethyl isobutyrate
<i>aldehydes</i>	ethyl lactate
iso-butyraldehyde	ethyl valerate
<i>alkanes</i>	γ -valerolactone
pentane	<i>furans and tetrahydrofurans</i>
hexane	tetrahydrofuran
cyclopentane	2-methyltetrahydrofuran
methylcyclohexane	<i>ketones</i>
<i>alkenes</i>	propanone
2-methyl-2-butene	2-butanone
pentene	3-methyl-2-butanone
hexene	2-pentanone
<i>aromatics</i>	3-pentanone
toluene	2,4-dimethyl-3-pentanone
<i>ethers</i>	cyclopentanone
diisopropyl ether	<i>multiple oxygen functionalities</i>
	tetrahydrofurfuryl alcohol
	ethyl levulinate
	butyl levulinate

Note S3 Exemplary minimization problem of objective reduction

The exemplary minimization problem of objective reduction has four objectives ($F = (f_1, f_2, f_3, f_4)^T$) and three Pareto-optimal solutions since no solution is dominated by any of the others (Figure S1A). If objective f_4 is omitted, all solutions are still non-dominated in the reduced objective space ($F'_1 = (f_1, f_2, f_3)^T$), i.e., the Pareto dominance structure is preserved (Figure S1B). In this case, no error is induced by objective reduction because objective f_4 is redundant. However, if additionally objective f_3 is omitted ($F'_2 = (f_1, f_2)^T$), solution s2 is dominated by solution s3 (Figure S1C) although it was not dominated in the full objective space F . Consequently, solution s2 would be lost in F'_2 since it is no longer Pareto-optimal. Thus, the Pareto dominance structure of the full objective space is changed due to objective reduction. The so-called δ -error quantifies this change as the maximum amount that has to be subtracted from a solution, which is dominating another solution in a reduced objective space, to render this solution also dominating the other solution in the full objective space. In this exemplary minimization problem, the δ -error is 0.5: The value of solution s3 regarding objective f_3 has to be subtracted by 0.5 such that solution s3 would not only dominate solution s2 in the reduced objective space F'_2 but also in the full objective space F .

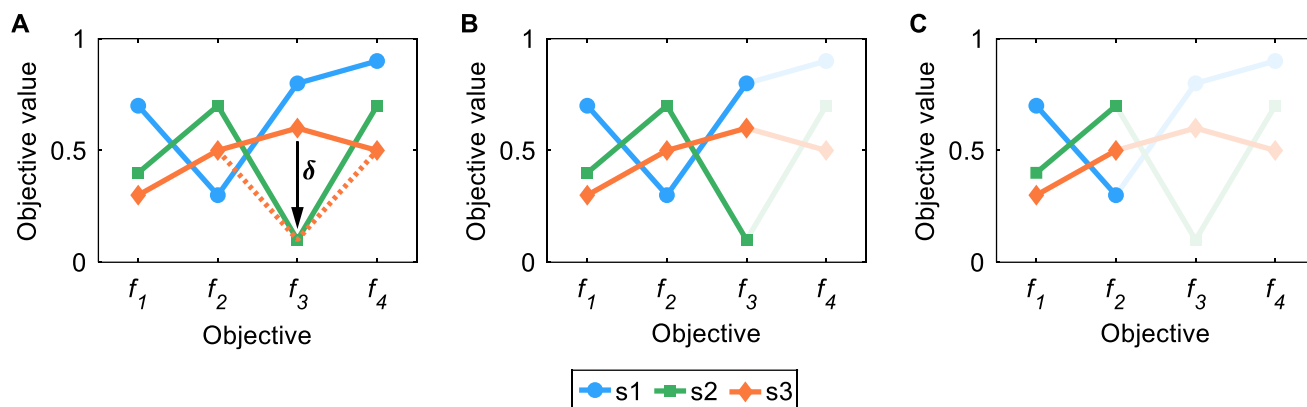


Figure S1: Dominance structures of (A) the full objective set $F = (f_1, f_2, f_3, f_4)^T$, (B) the reduced objective subset $F'_1 = (f_1, f_2, f_3)^T$, and (C) the reduced objective subset $F'_2 = (f_1, f_2)^T$, for an exemplary minimization problem. In (A) and (B), all solutions are Pareto-optimal while solution s3 dominates solution s2 in (C).

Note S4 Comparison with previous fuel design studies

In this study, we partly adjust the economic and environmental input data of utilities and feedstocks based on the study of König et al.²⁹ To analyze the implications of these adjustments, we compare the Pareto fronts for GWI and production cost using the input data of König et al. with using the input data of our 'today' scenario (Figure S2).

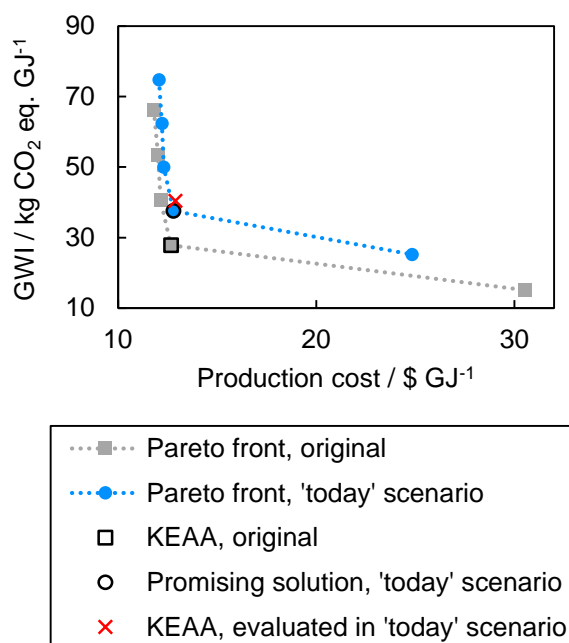


Figure S2: Pareto front with feedstock and utility data of König et al.²⁹ (grey) or the 'today' scenario of this study (blue). In König et al., the KEAA blend is a Pareto-optimal solution (square), whereas the KEAA blend is near-optimal when evaluated with this study's 'today' scenario (cross). Noteworthy, the most-promising solution of the 'today' scenario (circle) is also a KEAA blend but with slight changes in fuel composition.

Overall, we find similar trends using the input data of the 'today' scenario or König et al.²⁹ With our 'today' scenario, GWI values are slightly greater while production cost is almost equal except for the GWI-optimal solution: GWI scores increase by 9 to 10 kg CO₂ eq. GJ⁻¹, mainly due to changes in the modeled steam and refrigeration supply. The KEAA blend, a Pareto-optimal solution of König et al., is a near-optimal solution when evaluated with this study's 'today' scenario (cross, Figure S2). Noteworthy, the Pareto-optimal solution representing the most-promising compromise of GWI and production cost in the 'today' scenario (circle, Figure S2) is also a KEAA blend with the same fuel components but slight changes in composition compared to the KEAA blend identified by König et al. (Table S3).

Table S3: Molar composition of the KEAA blend of König et al.²⁹ and the most-promising compromise solution of the 'today' scenario (circle, Figure S2).

Blend component	KEAA blend	Most-promising compromise solution of the 'today' scenario
Ethanol	0.25	0.24
Methanol	0.02	0.10
Ethyl acetate	0.13	0.12
Methyl isopropyl ketone	0.40	0.38
Methyl acetate	0.16	0.13
Pentane	0.04	0.03

Note S5 Life cycle assessment: inventory data

The used LCA inventory datasets are listed for all feedstocks, utilities, solvents, and others in Table S4. Note that the LCA database ecoinvent does not provide inventory for each solvent. We thus list only those solvents for which datasets are available.

Table S4: LCA datasets of the life cycle inventory.

Flow	Unit	Dataset ^a	Reference	Year
<i>Feedstocks</i>				
Carbon dioxide	kg	Capture at steel plant Direct air capture ^b	von der Assen et al. ³⁰ Deutz et al. ³¹	2016 2021
Biomass	kg	DE: hardwood forestry, beech, sustainable forest management	ecoinvent 3.8, cut-off ³²	2021
Hydrogen	kg	Water electrolysis, polymer electrolyte membrane	Reuss et al. ³³	2017
<i>Utilities</i>				
Electricity	MJ	DE: market for electricity, medium voltage DE: electricity production, wind, 1-3MW turbine, onshore	ecoinvent 3.8, cut-off ³² ecoinvent 3.8, cut-off ³²	2021 2021
Heat	MJ	RER: steam production, as energy carrier, in chemical industry	ecoinvent 3.8, cut-off ³²	2021
Cooling water	kg	Electrode vessel, power-to-heat efficiency of 95%	Müller et al. ³⁴	2020
Refrigeration	MJ	DE: market for water, decarbonised Cryogenic cooler	ecoinvent 3.8, cut-off ³² Ladner et al. ³⁵	2021 2011
<i>Solvents^c and others</i>				
Dimethyl sulfoxide	kg	RER: dimethyl sulfoxide production	ecoinvent 3.8, cut-off ³²	2021
γ-butyrolactone	kg	RER: dehydrogenation of butan-1,4-diol	ecoinvent 3.8, cut-off ³²	2021
1,4-dioxane	kg	RER: dioxane production	ecoinvent 3.8, cut-off ³²	2021
Helium	kg	GLO: helium purification	ecoinvent 3.8, cut-off ³²	2021
Benzene	kg	RER: benzene production	ecoinvent 3.8, cut-off ³²	2021
1,2-dichloro-ethane	kg	RER: ethylene dichloride production	ecoinvent 3.8, cut-off ³²	2021
Chlorobenzene	kg	RER: benzene chlorination	ecoinvent 3.8, cut-off ³²	2021
Dichloro-methane	kg	RER: dichloromethane production	ecoinvent 3.8, cut-off ³²	2021
Chloroform	kg	RER: trichloromethane production	ecoinvent 3.8, cut-off ³²	2021
Cyclohexane	kg	RER: cyclohexane production	ecoinvent 3.8, cut-off ³²	2021
Gasoline	kg	RER: petrol production, low-sulfur ^d	ecoinvent 3.8, cut-off ³²	2021

^a Abbreviations in ecoinvent dataset names: DE: Germany; RER: Europe.

^b Energy requirements are taken from the predicted energy targets for a temperature-swing adsorption system.³¹ Heat is provided by heat pumps with a coefficient of performance (COP) of 3.28. The COP is averaged from heat pumps built since 2006 with condenser temperatures of about 90 °C and evaporator temperatures between 9-15 °C, according to David et al.³⁶

^c Solvents without available ecoinvent datasets are excluded from this list.

^d For gasoline, we assume a carbon content of 0.83 kg of carbon and a lower heating value of 41.3 MJ per kg to model combustion-induced CO₂ emissions.

Note S6 Influence of the number of Pareto points used as input for objective reduction

In Figure S3, we evaluate the influence of the number of Pareto points used as input for objective reduction exemplary for the ‘today’ scenario and normalization variant N2. For this analysis, we doubled the number of Pareto points used for objective reduction by increasing the resolution from four (N2) to eight (N2*) partitions per objective pair during Step 1 of the solution procedure (see Section 3.2). Overall, the influence of the number of Pareto points on the δ -error is negligible, with the highest increase observed for twelve omitted objectives (Figure S3). Notable, we still find the same reduced objective subsets $F_{OB=14}^{N2^*,today} = F_{OB=14}^{N2,today} = (C, LU, RU_m)^T$ for both N2* and N2. Consequently, in our case study, the objective reduction approach is not affected by this increase of the number of Pareto points. However, the computation time increases substantially by factor 2.3 (Table S5).

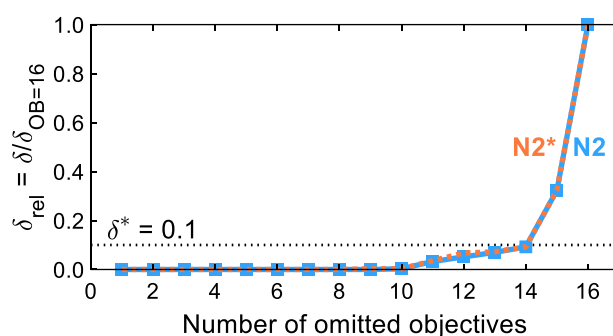


Figure S3: The δ -error δ_{rel} as function of the number of omitted objectives for normalization variant N2 in the ‘today’ scenario. To analyze the influence of the number of Pareto points used as input for objective reduction, N2* depicts the results for twice as many Pareto points compared to N2 (see Section 3.2). The threshold δ^* of 0.1 is introduced to identify small objective subsets with acceptable δ -error.

Table S5: Comparison of the number of partitions and generated solutions as well as the computation time.

Variant	Number of partitions	Initial solutions $S_{initial}$	Filtered solutions $S_{filtered}$	Computation time of objection reduction / h
N2	4	544	156	13.97
N2*	8	1087	264	32.67

Note S7 Correlation matrices

In Table S10 and Table S11, we present the correlation matrices of the initial Pareto-optimal solutions $S_{\text{filtered}}^{\text{today}}$ and $S_{\text{filtered}}^{\text{future}}$ for the 'today' and 'future' scenario, respectively. In the 'today' scenario, land use (LU) is most conflicting with all other objectives while production cost (C) and freshwater eutrophication (E_{fw}) show, on average, the weakest correlation with the other objectives. In the 'future' scenario, LU and E_{fw} are both conflicting with the other objectives, whereas C shows, again, only a slight correlation. The correlation matrices indicate correlation between all other objectives.

Note S8 Optimal process and fuel designs for the reduced objective subset

In Figure S4, we present the single-objective minima of the Pareto-optimal solutions generated with the reduced objective subsets. Figure S5 presents Pareto-optimal process and fuel designs of bio-fuels generated in the 'future' scenario that yield lower scores than the benchmark KEAA in all objectives.

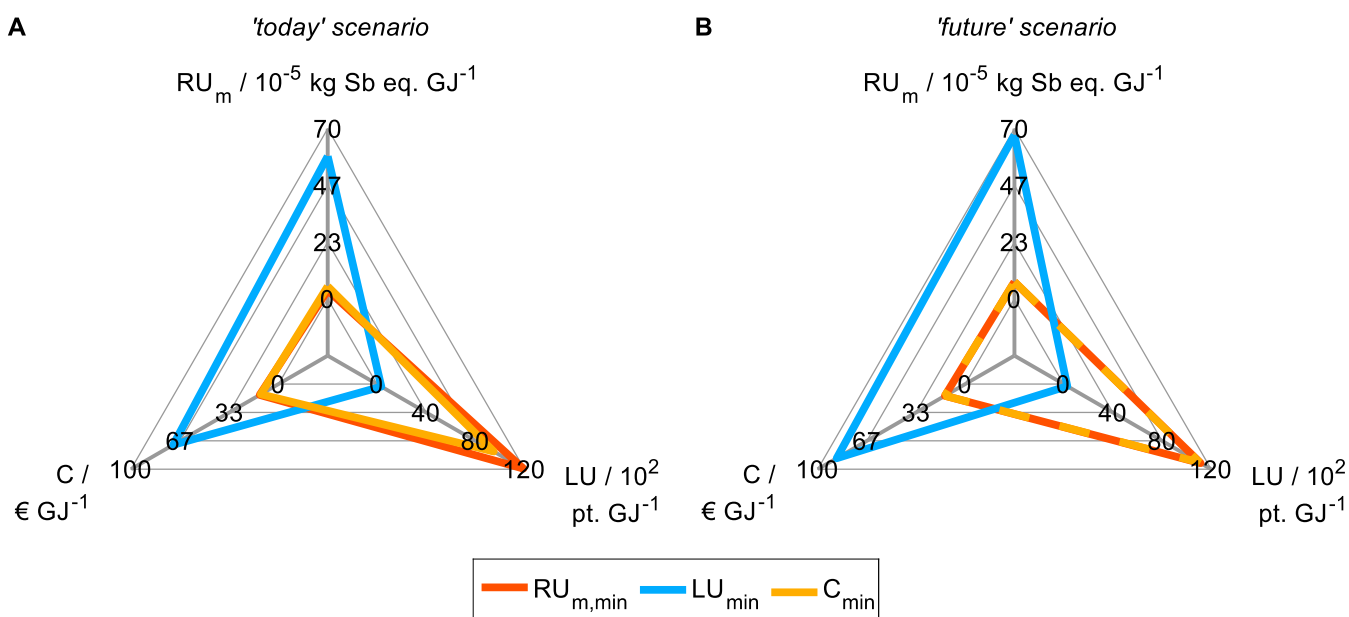


Figure S4: Pareto-optimal process and fuel designs regarding the reduced objective space of the (A) 'today' and (B) 'future' scenario. For each of these objectives, the optimum is shown, i.e., the design with minimum production cost (C), resource use of minerals and metals (RU_m), and land use (LU).

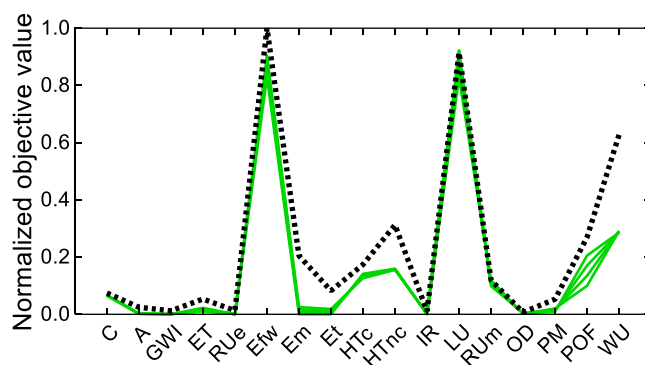


Figure S5: Pareto-optimal process and fuel designs of bio-fuels (green) generated for the 'future' scenario and evaluated in the full objective space. All of the depicted bio-fuels yield lower scores than the KEAA benchmark (dotted) in all objectives. Each objective is normalized according to normalization variant N1. Note that, for consistency, we recalculated the results of the KEAA blend of previous studies with our 'future' scenario.

Note S9 Contribution analysis

In Figure S6 to Figure S22, we present violin plots for relative contribution analyses regarding all 17 objectives. For these contribution analyses, we clustered the generated Pareto-optimal solutions of the reduced objective subsets by fuel type (bio-, e-, and bio-hybrid-fuel) for each scenario.

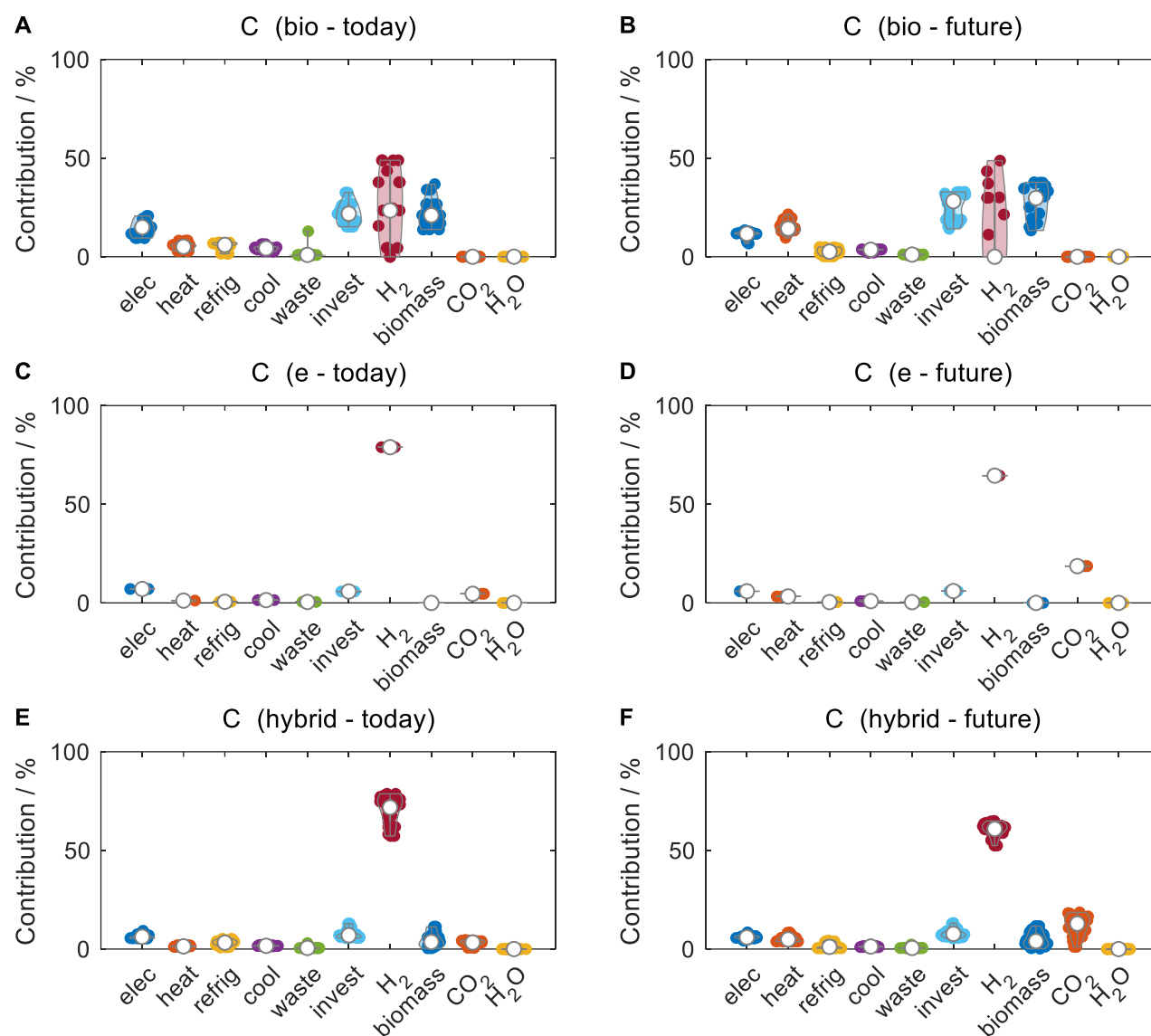


Figure S6: Violin plot for the relative contribution analysis regarding production cost of bio-, e-, and bio-hybrid fuels in the 'today' and 'future' scenario. For each subfigure, all Pareto-optimal solutions of the corresponding fuel type and scenario are considered that have been generated for the reduced objective subset.

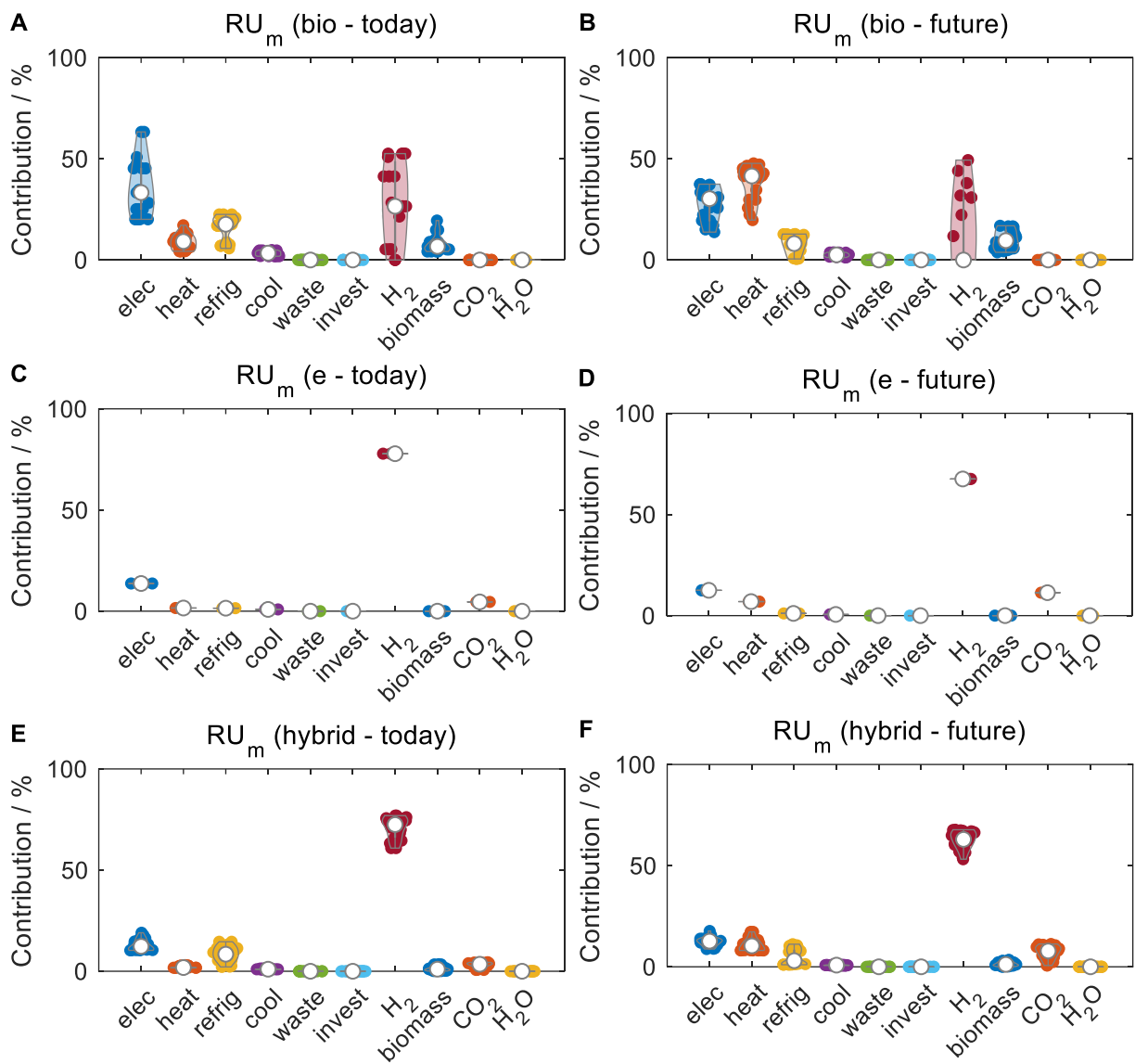


Figure S7: Violin plot for the relative contribution analysis regarding resource use of minerals and metals of bio-, e-, and bio-hybrid fuels in the 'today' and 'future' scenario. For each subfigure, all Pareto-optimal solutions of the corresponding fuel type and scenario are considered that have been generated for the reduced objective subset.

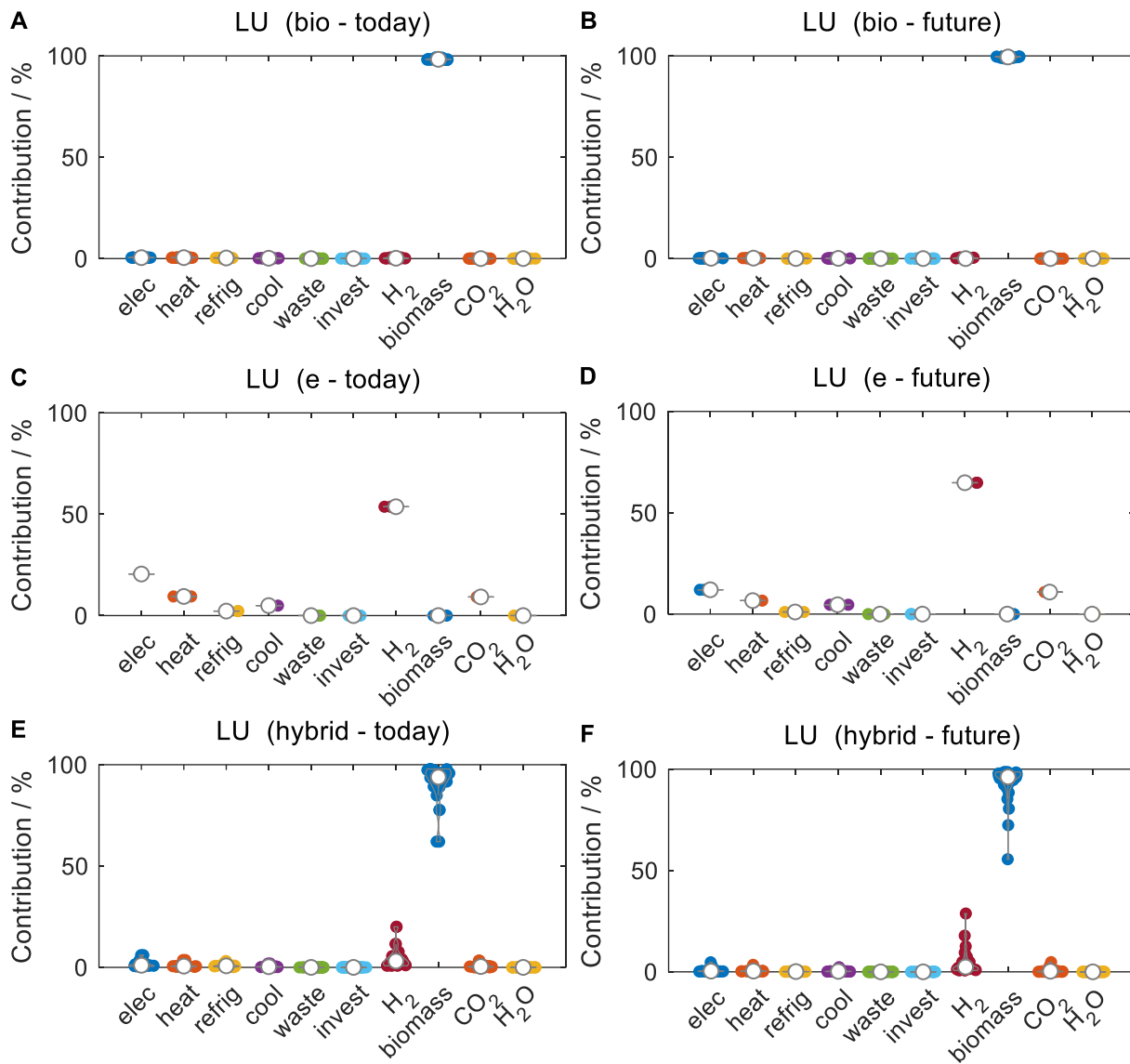


Figure S8: Violin plot for the relative contribution analysis regarding land use of bio-, e-, and bio-hybrid fuels in the ‘today’ and ‘future’ scenario. For each subfigure, all Pareto-optimal solutions of the corresponding fuel type and scenario are considered that have been generated for the reduced objective subset.

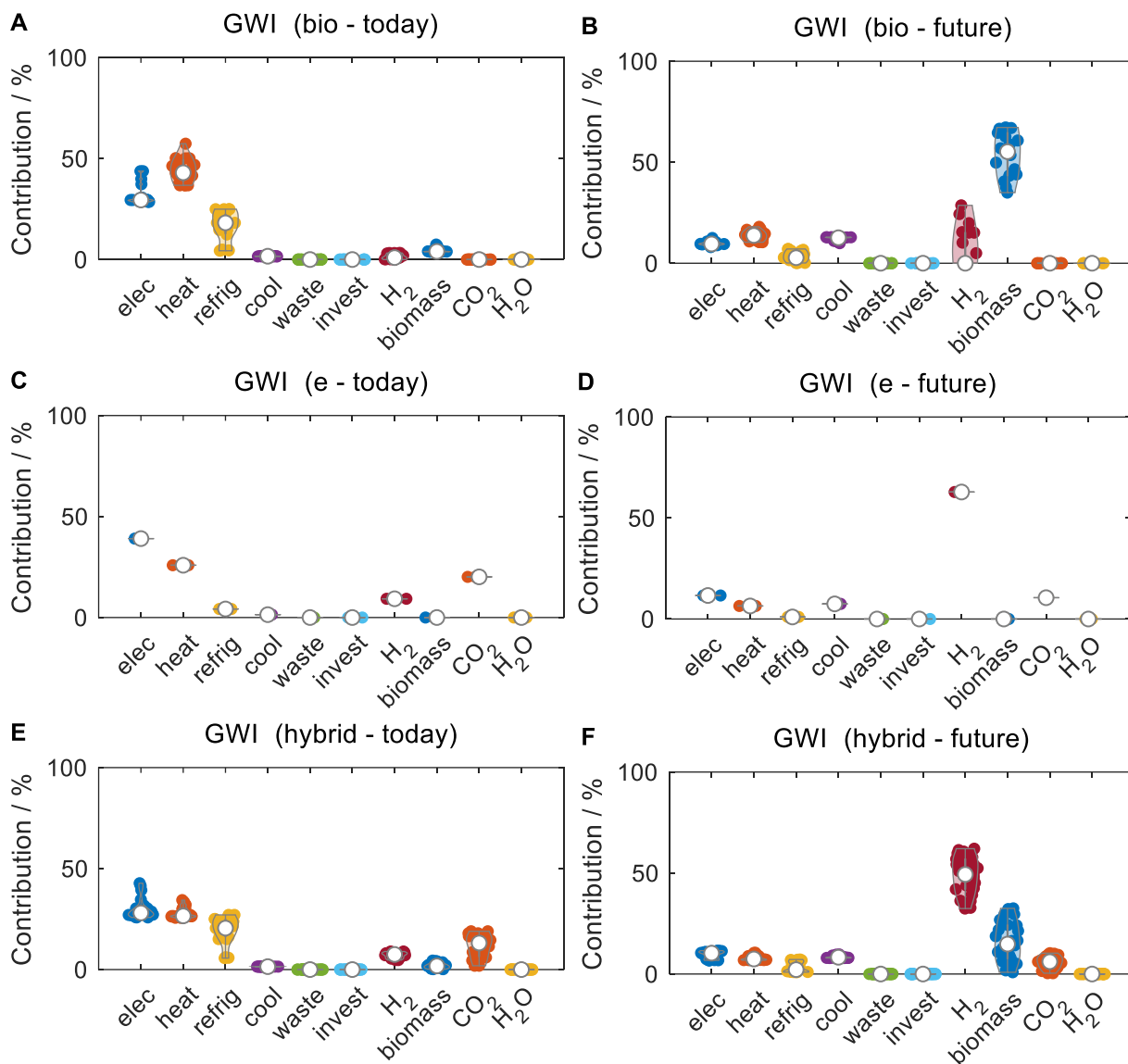


Figure S9: Violin plot for the relative contribution analysis regarding global warming impact of bio-, e-, and bio-hybrid fuels in the 'today' and 'future' scenario. For each subfigure, all Pareto-optimal solutions of the corresponding fuel type and scenario are considered that have been generated for the reduced objective subset.

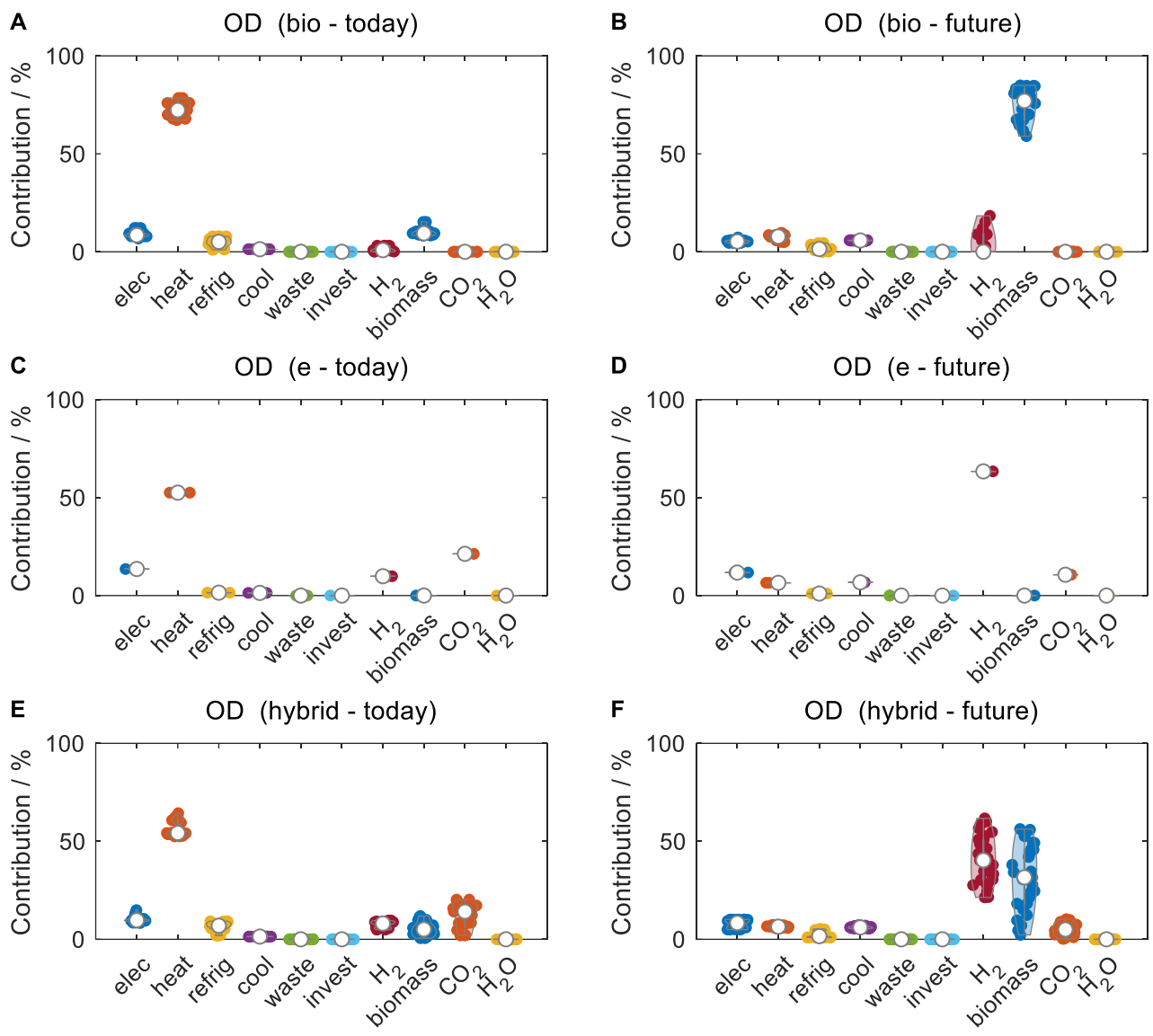


Figure S10: Violin plot for the relative contribution analysis regarding ozone depletion of bio-, e-, and bio-hybrid fuels in the 'today' and 'future' scenario. For each subfigure, all Pareto-optimal solutions of the corresponding fuel type and scenario are considered that have been generated for the reduced objective subset.

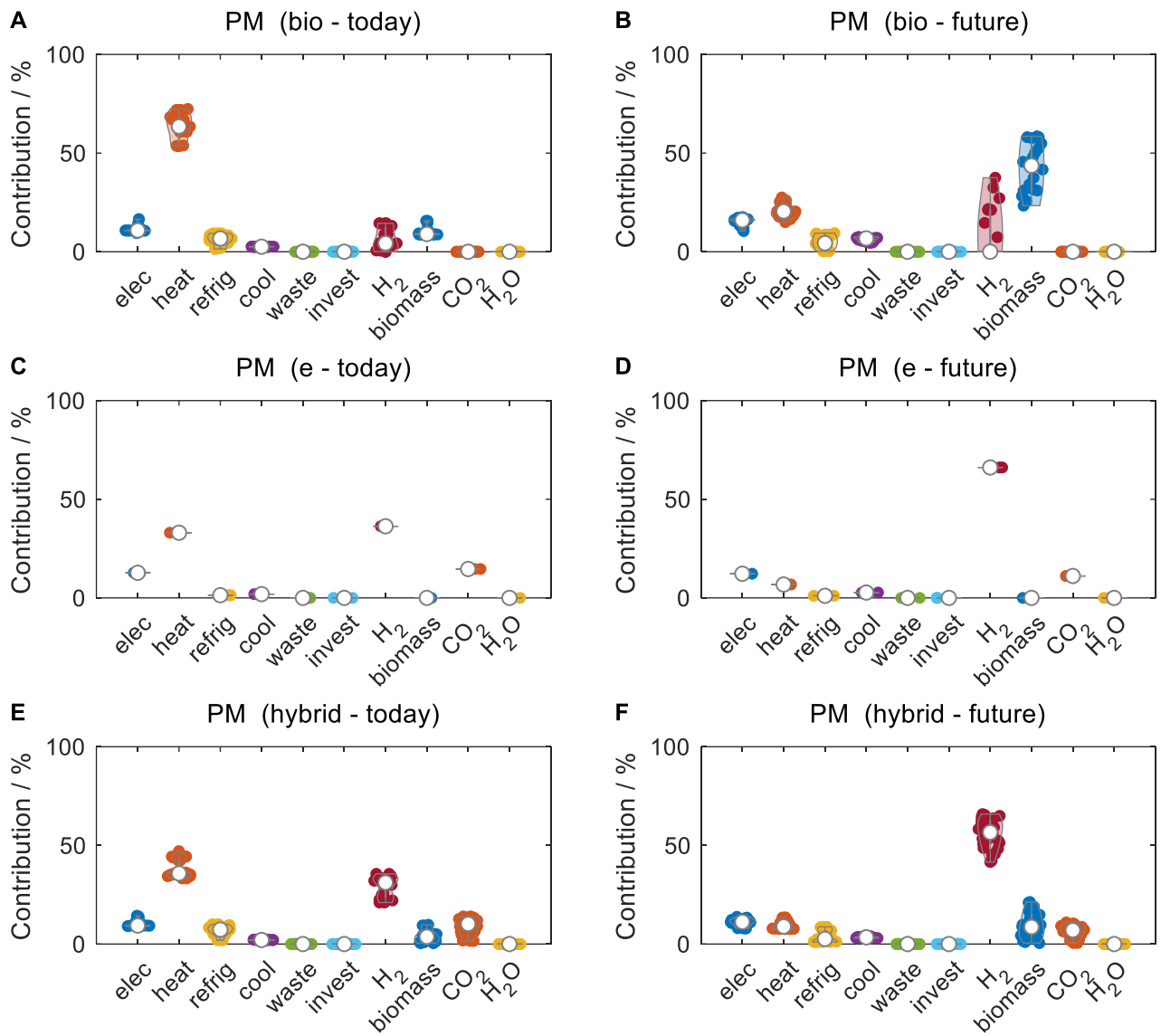


Figure S11: Violin plot for the relative contribution analysis regarding particulate matter of bio-, e-, and bio-hybrid fuels in the 'today' and 'future' scenario. For each subfigure, all Pareto-optimal solutions of the corresponding fuel type and scenario are considered that have been generated for the reduced objective subset.

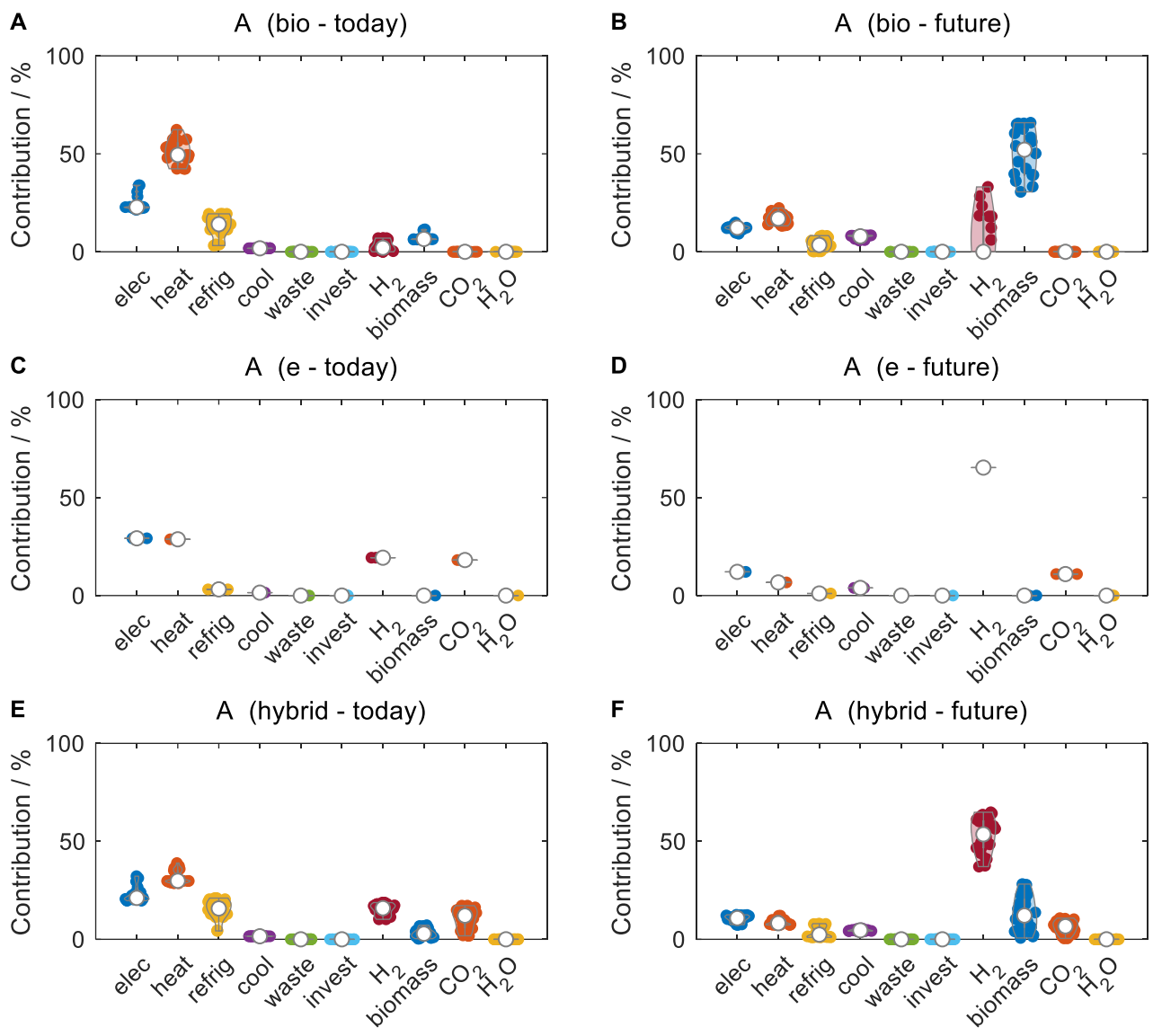


Figure S12: Violin plot for the relative contribution analysis regarding acidification of bio-, e-, and bio-hybrid fuels in the 'today' and 'future' scenario. For each subfigure, all Pareto-optimal solutions of the corresponding fuel type and scenario are considered that have been generated for the reduced objective subset.

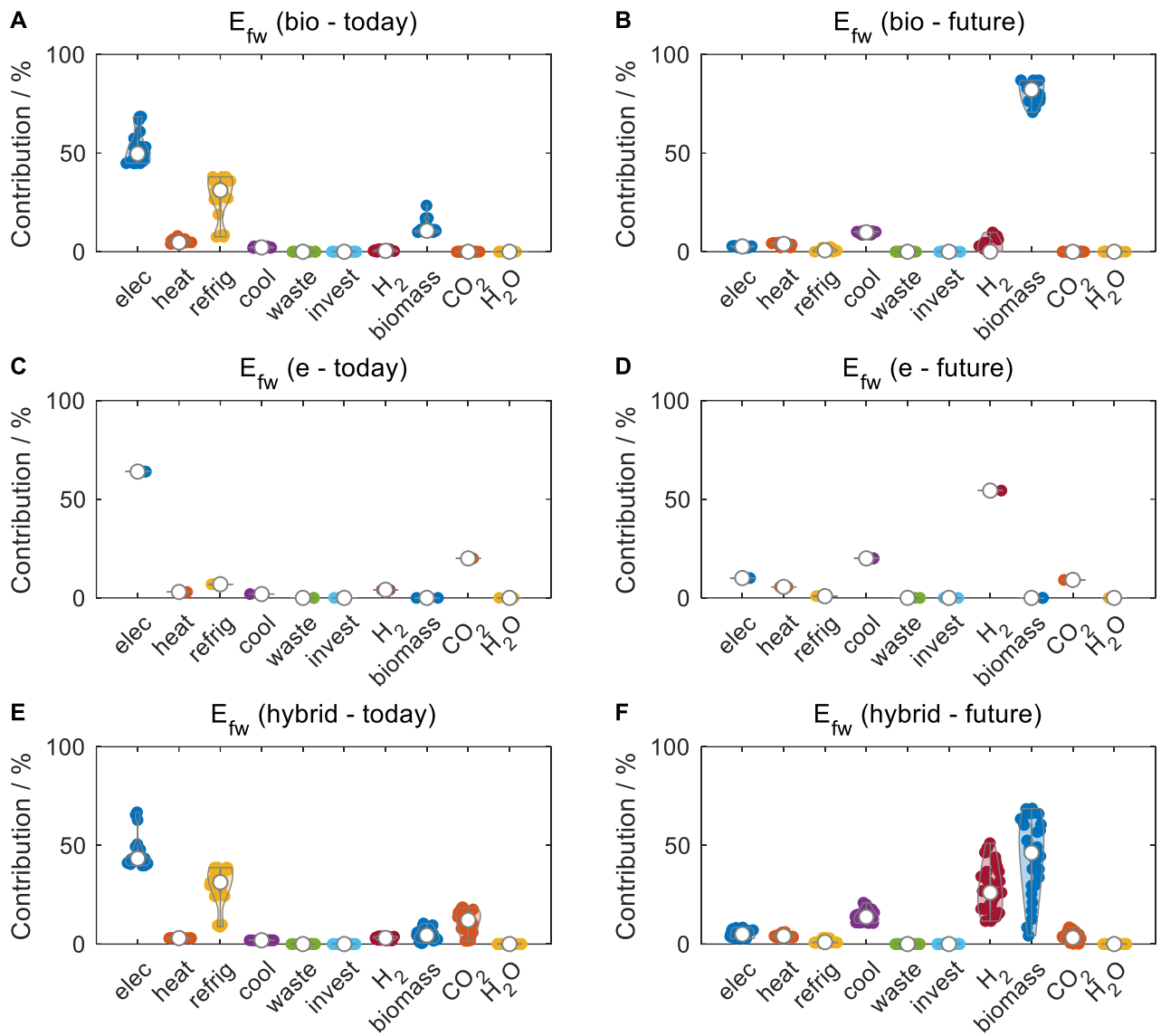


Figure S13: Violin plot for the relative contribution analysis regarding freshwater eutrophication of bio-, e-, and bio-hybrid fuels in the 'today' and 'future' scenario. For each subfigure, all Pareto-optimal solutions of the corresponding fuel type and scenario are considered that have been generated for the reduced objective subset.

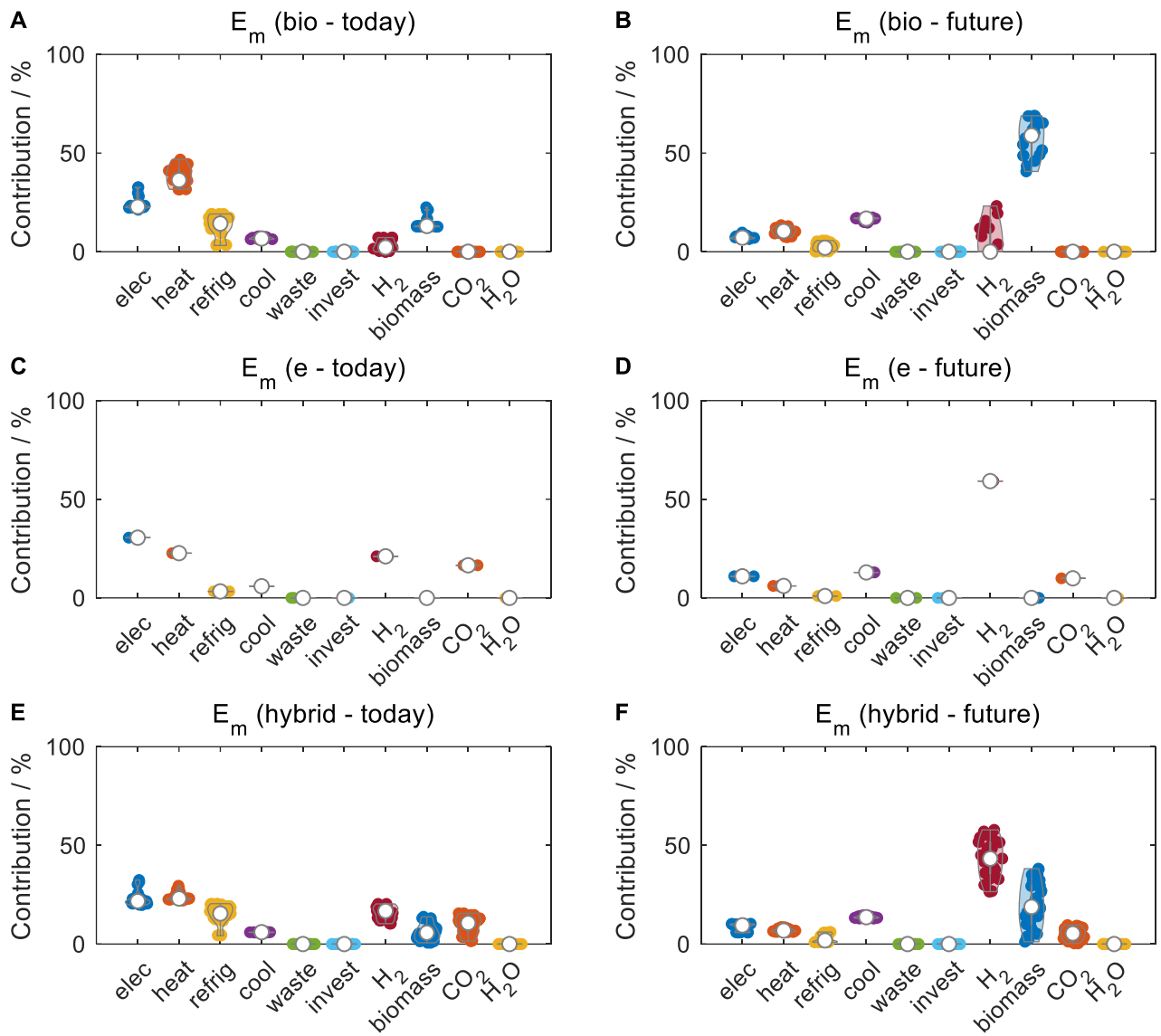


Figure S14: Violin plot for the relative contribution analysis regarding marine eutrophication of bio-, e-, and bio-hybrid fuels in the 'today' and 'future' scenario. For each subfigure, all Pareto-optimal solutions of the corresponding fuel type and scenario are considered that have been generated for the reduced objective subset.

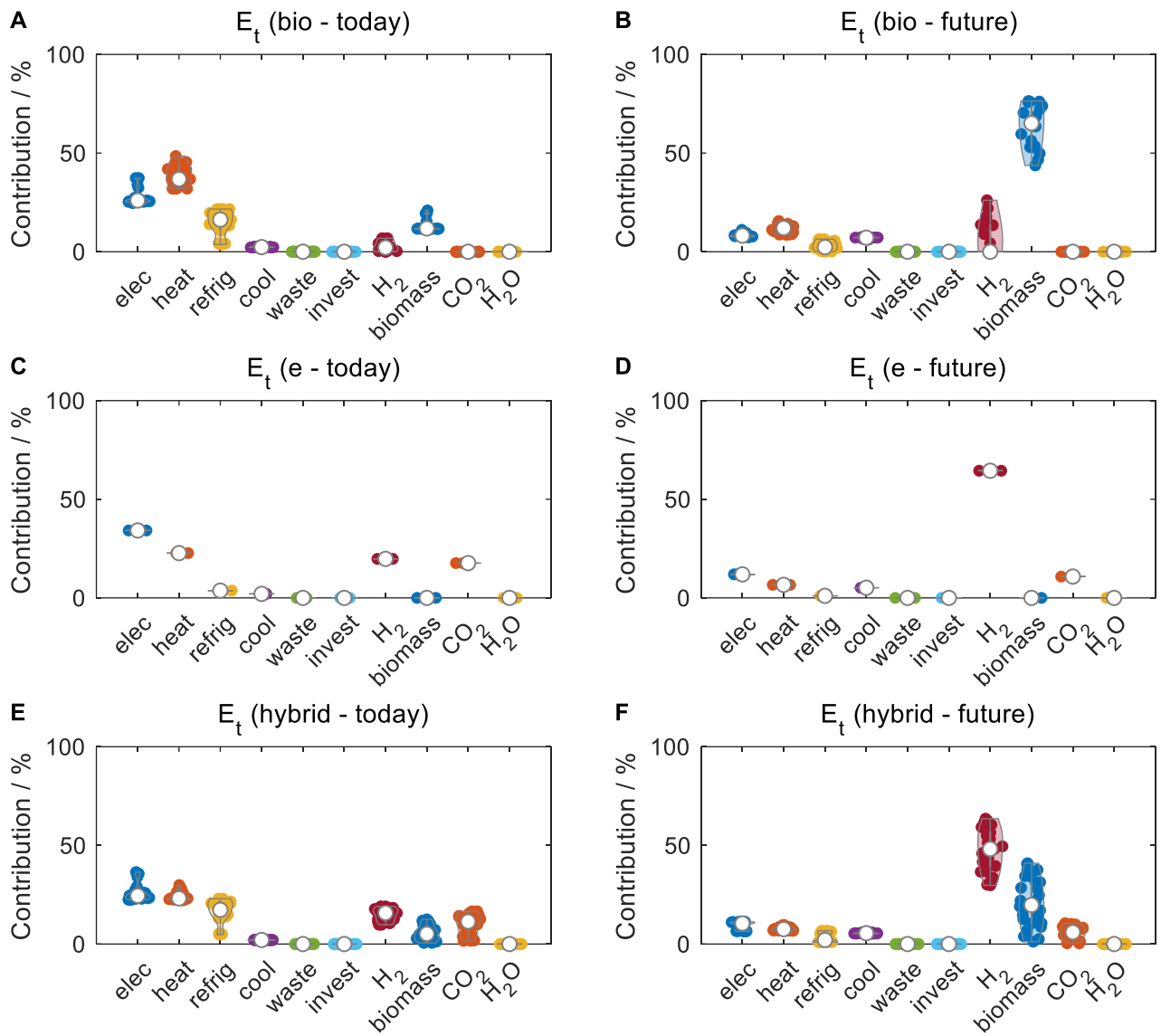


Figure S15: Violin plot for the relative contribution analysis regarding terrestrial eutrophication of bio-, e-, and bio-hybrid fuels in the 'today' and 'future' scenario. For each subfigure, all Pareto-optimal solutions of the corresponding fuel type and scenario are considered that have been generated for the reduced objective subset.

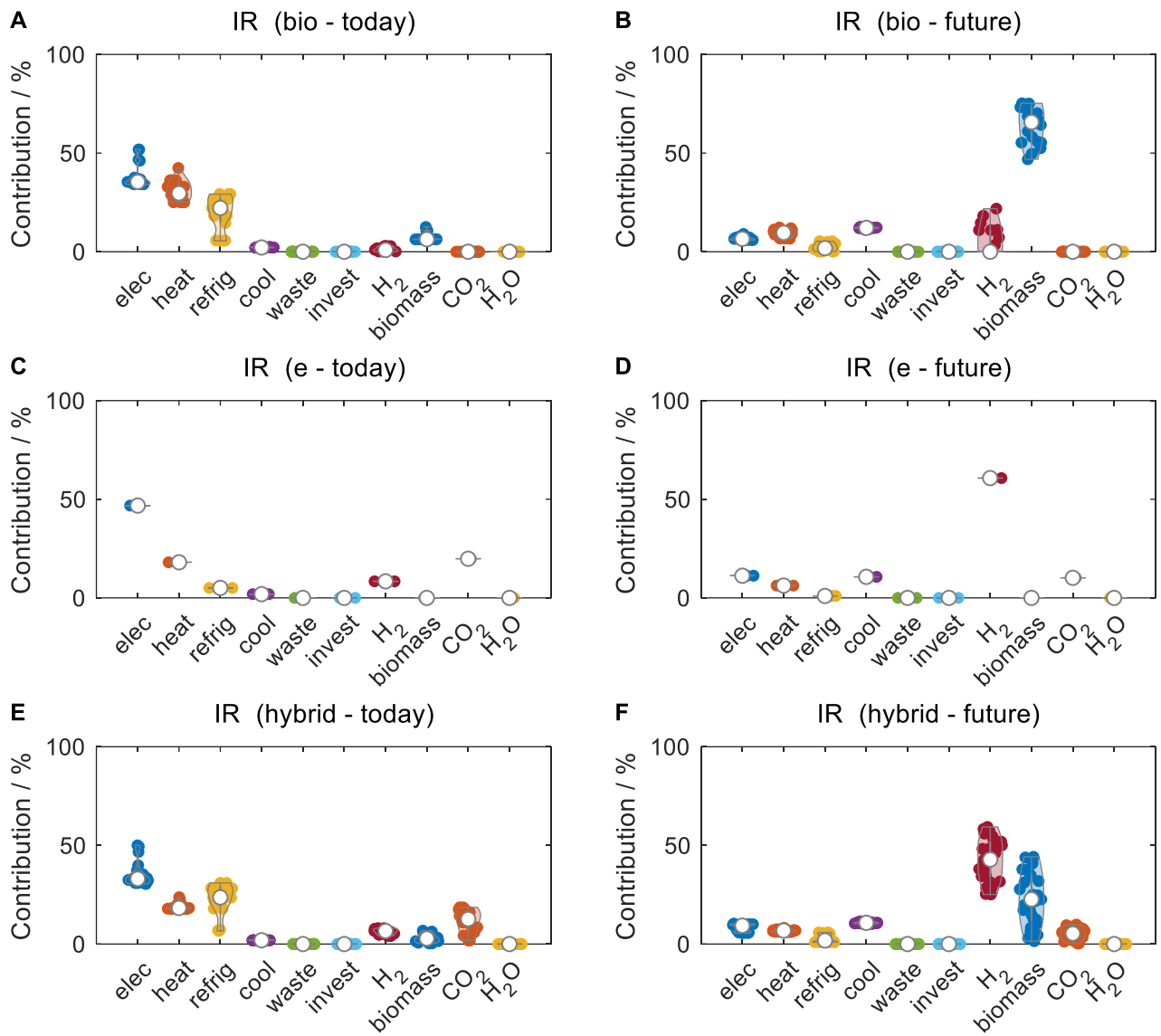


Figure S16: Violin plot for the relative contribution analysis regarding ionizing radiation of bio-, e-, and bio-hybrid fuels in the 'today' and 'future' scenario. For each subfigure, all Pareto-optimal solutions of the corresponding fuel type and scenario are considered that have been generated for the reduced objective subset.

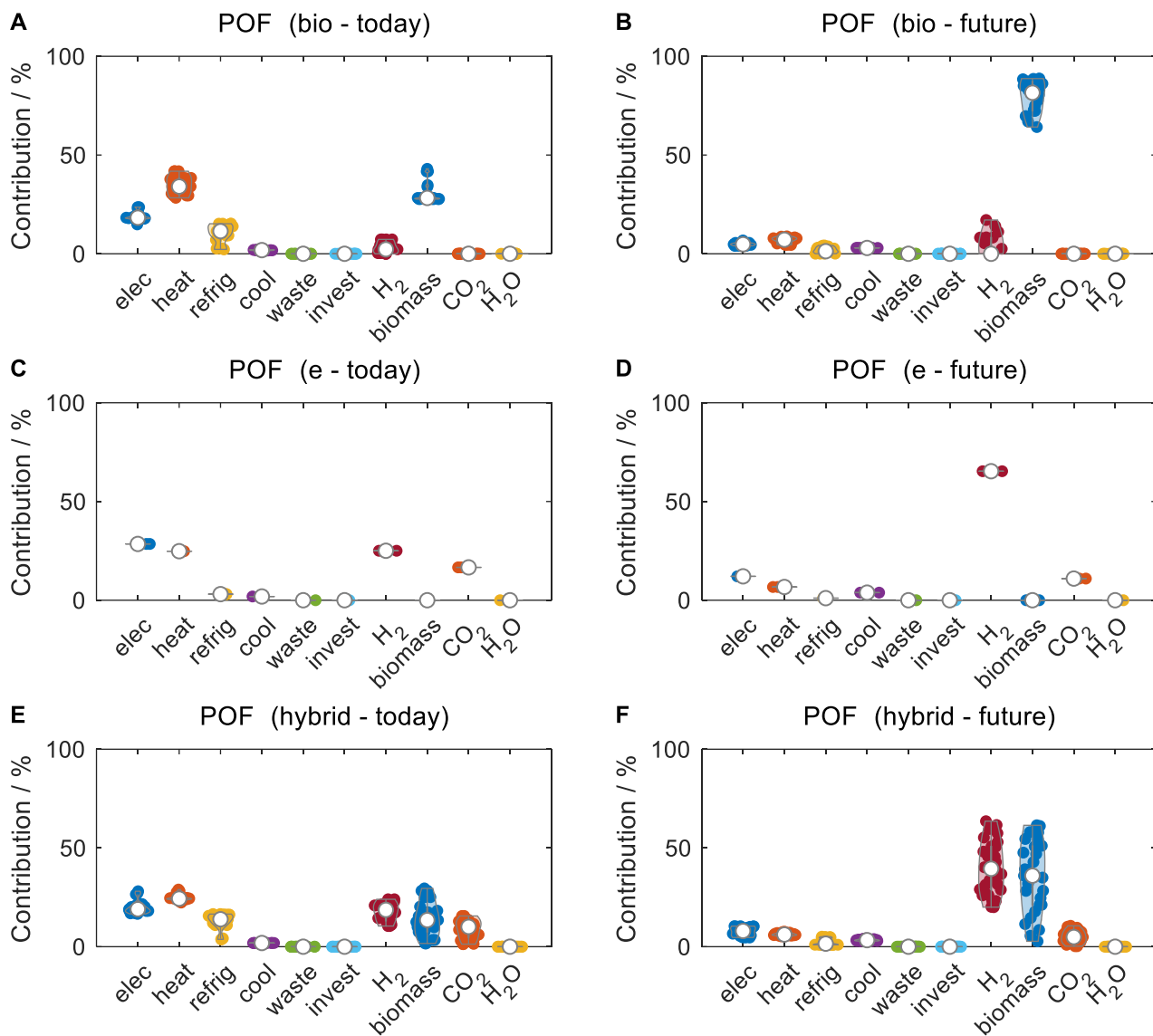


Figure S17: Violin plot for the relative contribution analysis regarding photochemical ozone formation of bio-, e-, and bio-hybrid fuels in the 'today' and 'future' scenario. For each subfigure, all Pareto-optimal solutions of the corresponding fuel type and scenario are considered that have been generated for the reduced objective subset.

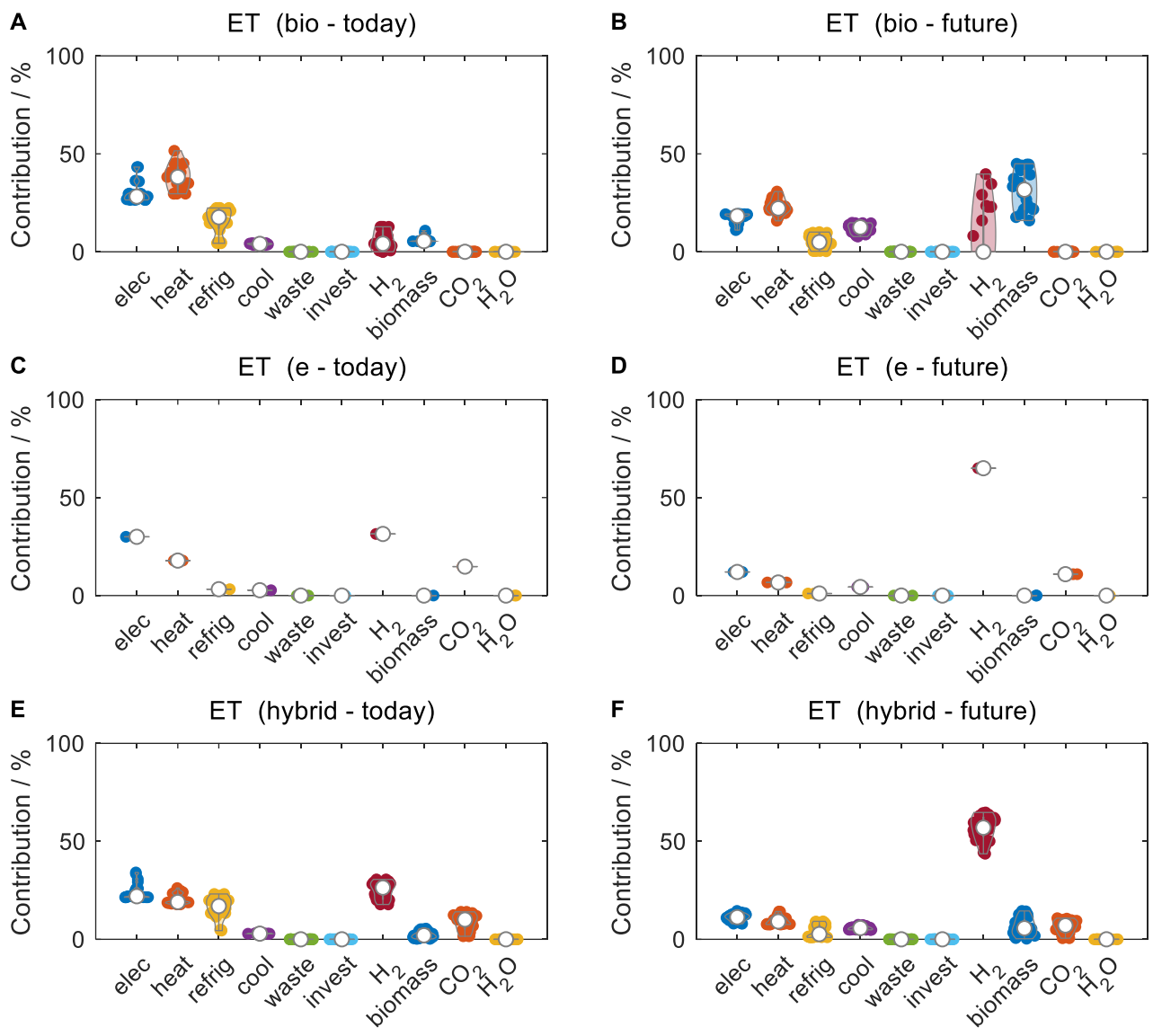


Figure S18: Violin plot for the relative contribution analysis regarding ecotoxicity of bio-, e-, and bio-hybrid fuels in the 'today' and 'future' scenario. For each subfigure, all Pareto-optimal solutions of the corresponding fuel type and scenario are considered that have been generated for the reduced objective subset.

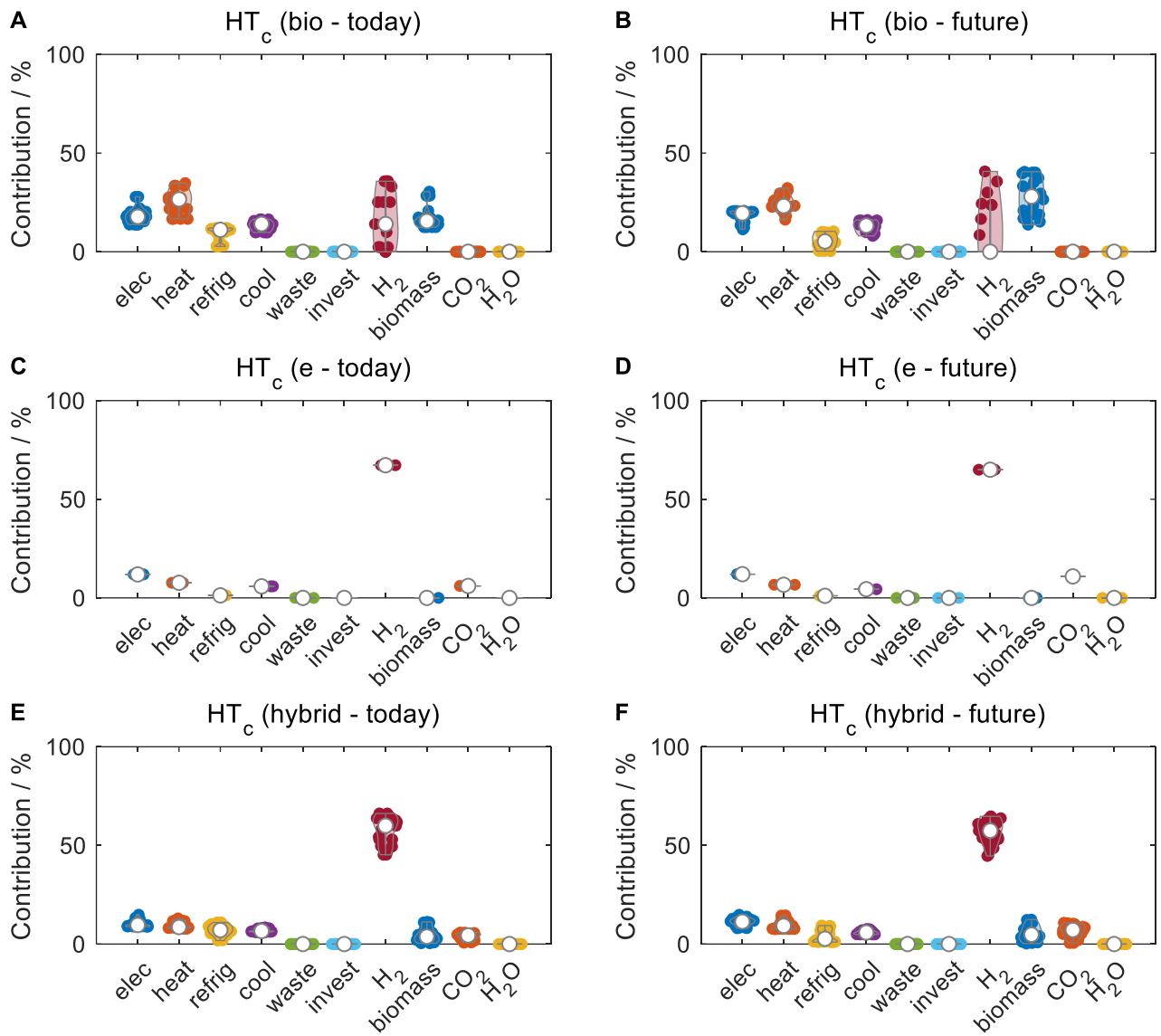


Figure S19: Violin plot for the relative contribution analysis regarding carcinogenic human toxicity of bio-, e-, and bio-hybrid fuels in the 'today' and 'future' scenario. For each subfigure, all Pareto-optimal solutions of the corresponding fuel type and scenario are considered that have been generated for the reduced objective subset.

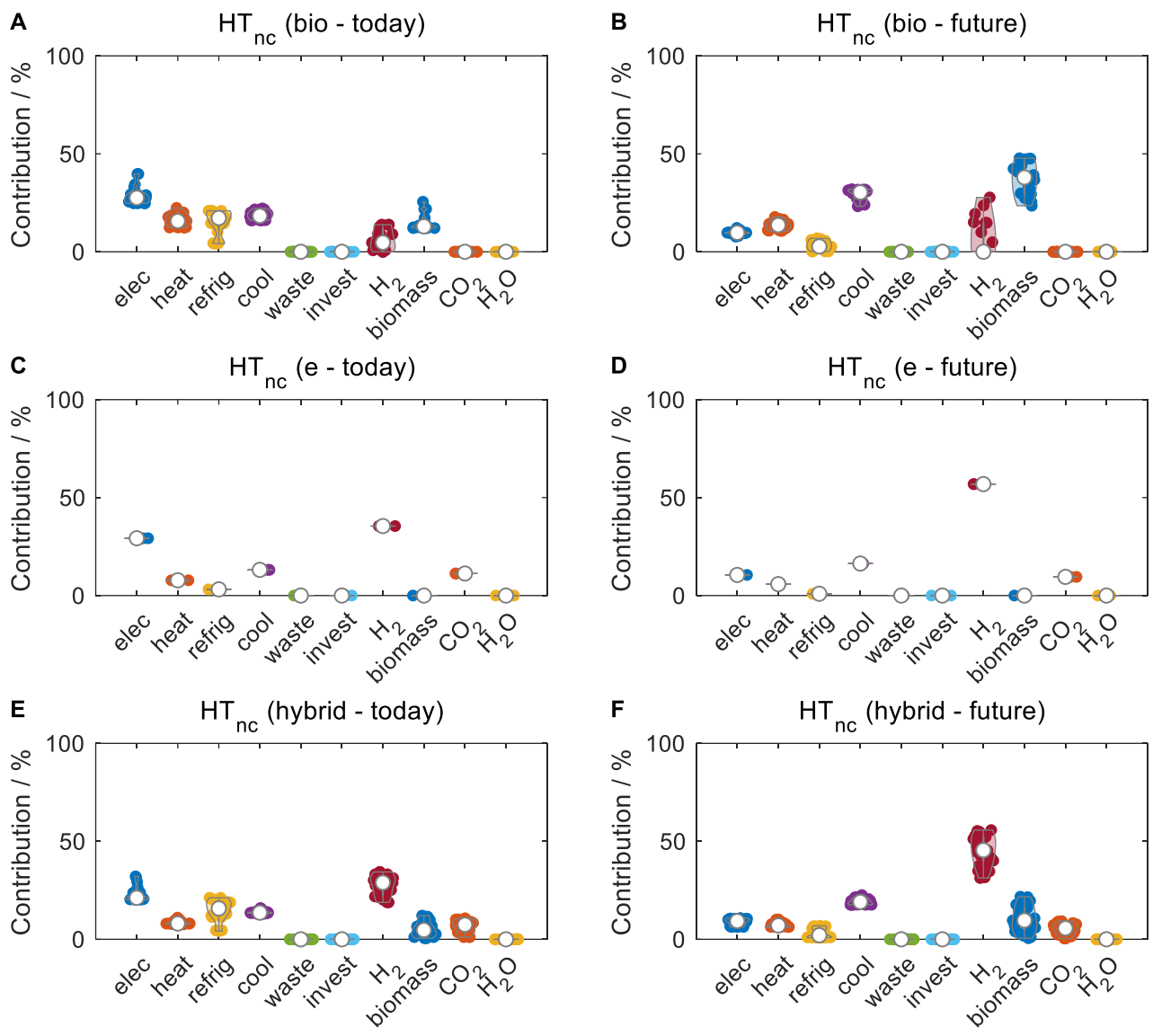


Figure S20: Violin plot for the relative contribution analysis regarding non-carcinogenic human toxicity of bio-, e-, and bio-hybrid fuels in the 'today' and 'future' scenario. For each subfigure, all Pareto-optimal solutions of the corresponding fuel type and scenario are considered that have been generated for the reduced objective subset.

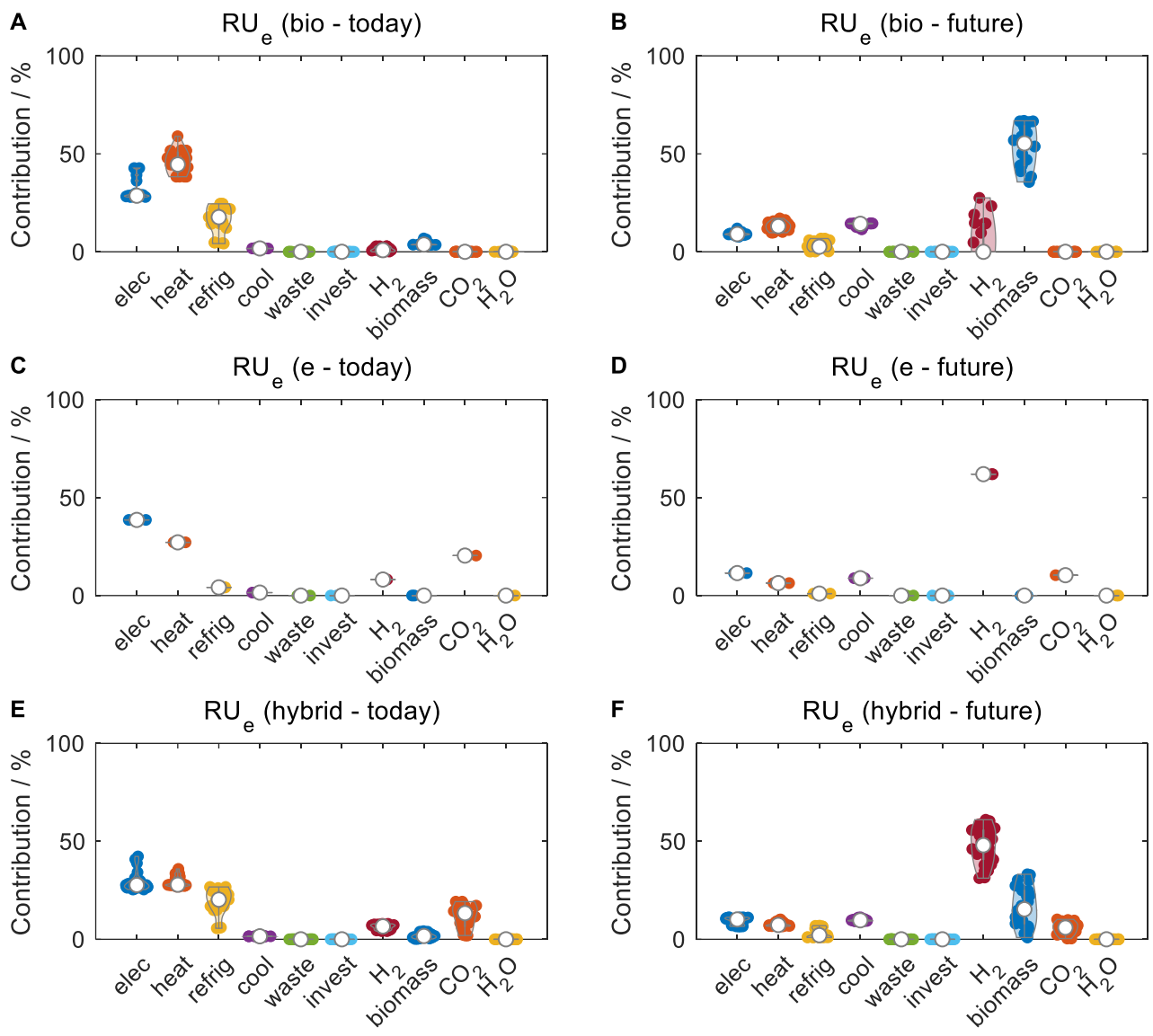


Figure S21: Violin plot for the relative contribution analysis regarding resource use of energy carriers of bio-, e-, and bio-hybrid fuels in the 'today' and 'future' scenario. For each subfigure, all Pareto-optimal solutions of the corresponding fuel type and scenario are considered that have been generated for the reduced objective subset.

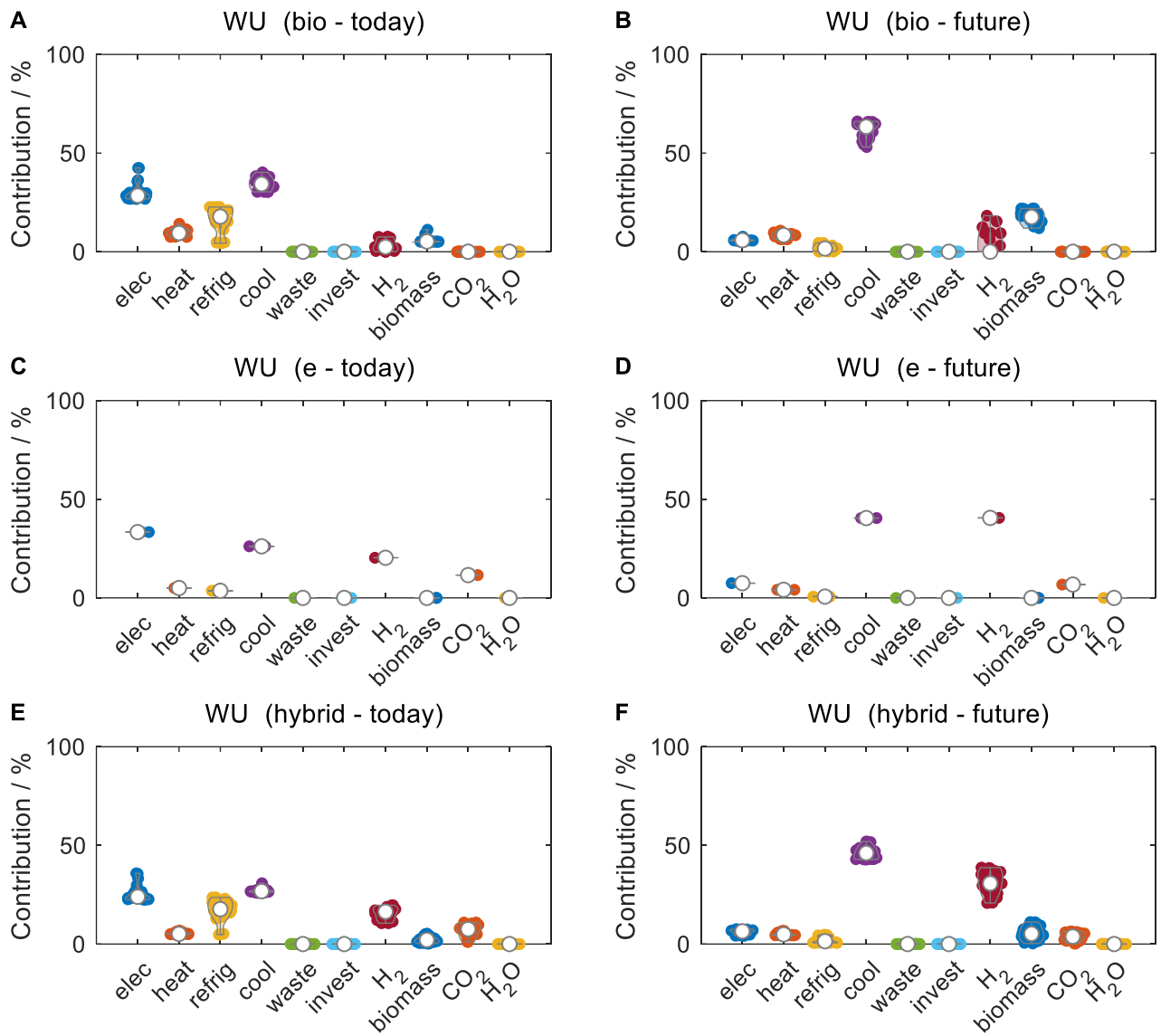


Figure S22: Violin plot for the relative contribution analysis regarding water use of bio-, e-, and bio-hybrid fuels in the 'today' and 'future' scenario. For each subfigure, all Pareto-optimal solutions of the corresponding fuel type and scenario are considered that have been generated for the reduced objective subset.

Note S10 Composition of Pareto-optimal bio-hybrid fuels

In Figure S23, we show the molar fuel composition of all generated Pareto-optimal bio-hybrid fuels as violin plot. For comparison, we also present the molar composition of the KEAA blend of previous studies.²⁹

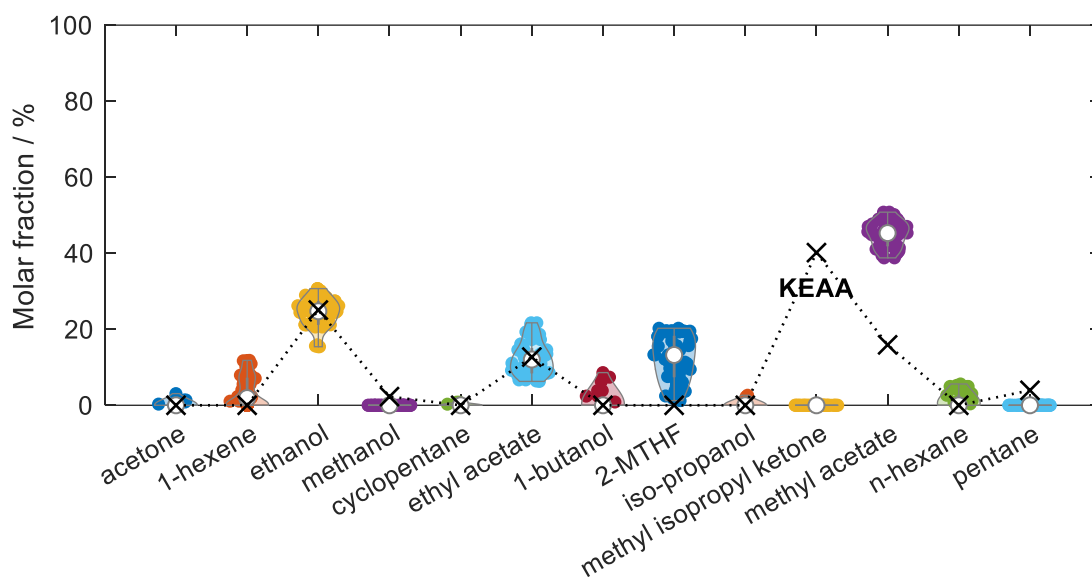


Figure S23: Violin plot for the molar composition of all generated Pareto-optimal bio-hybrid fuels. For comparison, the molar composition of the KEAA blend of previous studies is shown as crosses.²⁹ MTHF: methyltetrahydrofuran.

Supplementary references

1. G. Guillén-Gosálbez, *Computers & Chemical Engineering*, 2011, **35** (8), 1469.
2. D. Brockhoff and E. Zitzler in *Parallel Problem Solving from Nature - PPSN IX: 9th International Conference, Reykjavik, Iceland, September 9-13, 2006, Proceedings*, ed. D. Hutchison, T. Kanade, J. Kittler, J. M. Kleinberg, F. Mattern, J. C. Mitchell, M. Naor, O. Nierstrasz, C. Pandu Rangan, B. Steffen, M. Sudan, D. Terzopoulos, D. Tygar, M. Y. Vardi, G. Weikum, T. P. Runarsson, H.-G. Beyer, E. Burke, J. J. Merelo-Guervós, L. D. Whitley, X. Yao and E. K. Burke, Springer Berlin Heidelberg, Berlin, Heidelberg, 2006, p 533.
3. Y. J. Qin, J. H. Zheng, Z. Li and Q. H. Wu, *International Journal of Electrical Power & Energy Systems*, 2020, **117**, 105657.
4. K. Chu, W. Liu, Y. She, Z. Hua, M. Tan, X. Liu, L. Gu and Y. Jia, *Water*, 2018, **10** (1), 69.
5. J. R. Perez-Gallardo, C. Azzaro-Pantel and S. Astier, *Sustainable Energy Technologies and Assessments*, 2018, **27**, 94.
6. D. Vázquez, R. Ruiz-Femenia, L. Jiménez and J. A. Caballero, *Computers & Chemical Engineering*, 2018, **115**, 323.
7. D. Vázquez, R. Ruiz-Femenia, L. Jiménez and J. A. Caballero, *Ind. Eng. Chem. Res.*, 2018, **57** (20), 6992.
8. D. Vázquez, M. J. Fernández-Torres, R. Ruiz-Femenia, L. Jiménez and J. A. Caballero, *Computers & Chemical Engineering*, 2018, **108**, 382.
9. M. Hennen, S. Postels, P. Voll, M. Lampe and A. Bardow, *Computers & Chemical Engineering*, 2017, **97**, 283.
10. J. Wheeler, J. A. Caballero, R. Ruiz-Femenia, G. Guillén-Gosálbez and F. D. Mele, *Computers & Chemical Engineering*, 2017, **102** (4), 64.
11. J. Carreras, C. Pozo, D. Boer, G. Guillén-Gosálbez, J. A. Caballero, R. Ruiz-Femenia and L. Jiménez, *Energy and Buildings*, 2016, **130** (3), 506.
12. P. J. Copado-Méndez, C. Pozo, G. Guillén-Gosálbez and L. Jiménez, *Computers & Chemical Engineering*, 2016, **87**, 36.
13. Z. J. N. Steinmann, A. M. Schipper, M. Hauck and M. A. J. Huijbregts, *Environmental science & technology*, 2016, **50** (7), 3913.
14. A. Kostin, G. Guillén-Gosálbez and L. Jiménez, *International Journal of Production Economics*, 2015, **159**, 223.
15. S. Postels, N. von der Assen, P. Voll and A. Bardow in *28th International Conference on Efficiency, Cost, Optimization, Simulation and Environmental Impact of Energy Systems (ECOS 2015): Pau, France, 30 June-3 July 2015*, Curran Associates Inc, Red Hook, NY, 2015, p 787.
16. P. J. Copado-Méndez, G. Guillén-Gosálbez and L. Jiménez, *Computers & Chemical Engineering*, 2014, **67** (19), 137.
17. L. Čuček, J. J. Klemeš and Z. Kravanja, *Journal of Cleaner Production*, 2014, **71**, 75.
18. P. Vaskan, G. Guillén-Gosálbez, M. Turkyay and L. Jiménez, *Ind. Eng. Chem. Res.*, 2014, **53** (50), 19559.
19. E. Antipova, D. Boer, L. F. Cabeza, G. Guillén-Gosálbez and L. Jiménez, *Energy*, 2013, **51**, 50.
20. D. G. Oliva, G. Guillén-Gosálbez, J. M. Mateo-Sanz and L. Jiménez-Esteller, *Computers & Chemical Engineering*, 2013, **56**, 202.

21. R. Brunet, G. Guillén-Gosálbez and L. Jiménez, *Ind. Eng. Chem. Res.*, 2012, **51** (1), 410.
22. A. Kostin, G. Guillén-Gosálbez, F. D. Mele and L. Jiménez, *Ind. Eng. Chem. Res.*, 2012, **51** (14), 5282.
23. C. Pozo, R. Ruíz-Femenia, J. Caballero, G. Guillén-Gosálbez and L. Jiménez, *Chemical Engineering Science*, 2012, **69** (1), 146.
24. N. Sabio, A. Kostin, G. Guillén-Gosálbez and L. Jiménez, *International Journal of Hydrogen Energy*, 2012, **37** (6), 5385.
25. P. Vaskan, G. Guillén-Gosálbez and L. Jiménez, *Applied Energy*, 2012, **98**, 149.
26. E. Gutiérrez, S. Lozano and B. Adenso-Díaz, *Journal of Industrial Ecology*, 2010, **14** (6), 878.
27. K. Ulonska, M. Skiborowski, A. Mitsos and J. Viell, *AIChE J.*, 2016, **62** (9), 3096.
28. A. König, L. Neidhardt, J. Viell, A. Mitsos and M. Dahmen, *Computers & Chemical Engineering*, 2020, **134**, 106712.
29. A. König, M. Siska, A. M. Schweidtmann, J. G. Rittig, J. Viell, A. Mitsos and M. Dahmen, *Chemical Engineering Science*, 2021, **237**, 116562.
30. N. von der Assen, L. J. Müller, A. Steingrube, P. Voll and A. Bardow, *Environmental science & technology*, 2016, **50** (3), 1093.
31. S. Deutz and A. Bardow, *Nat Energy*, 2021, **6**, 203.
32. G. Wernet, C. Bauer, B. Steubing, J. Reinhard, E. Moreno-Ruiz and B. Weidema, *Int J Life Cycle Assess*, 2016, **21** (9), 1218.
33. M. Reuß, T. Grube, M. Robinius, P. Preuster, P. Wasserscheid and D. Stolten, *Applied Energy*, 2017, **200**, 290.
34. L. J. Müller, A. Kätelhön, M. Bachmann, A. Zimmermann, A. Sternberg and A. Bardow, *Front. Energy Res.*, 2020, **8**, 1.
35. D. R. Ladner in *Cryocoolers 16: International Cryocooler Conference 16, Atlanta, GA, ICC 16 ; proceedings of the 16th ICC, Atlanta, GA, May 17 - 20, 2010*, ed. S. D. Miller, ICC Press, Boulder, Colo., 2011.
36. A. David, B. V. Mathiesen, H. Averfalk, S. Werner and H. Lund, *Energies*, 2017, **10** (4), 578.